

Paint Outside the Box: Synthesizing and Selecting Training Data for Visual Grounding

Zilin Du

zilin003@e.ntu.edu.sg

Nanyang Technological University
Singapore

Jianfei Yu

jfyu@njust.edu.cn

Nanjing University of Science and Technology
China

Haoxin Li

haoxin003@e.ntu.edu.sg

Nanyang Technological University
Singapore

Boyang Li

boyang.li@ntu.edu.sg

Nanyang Technological University
Singapore

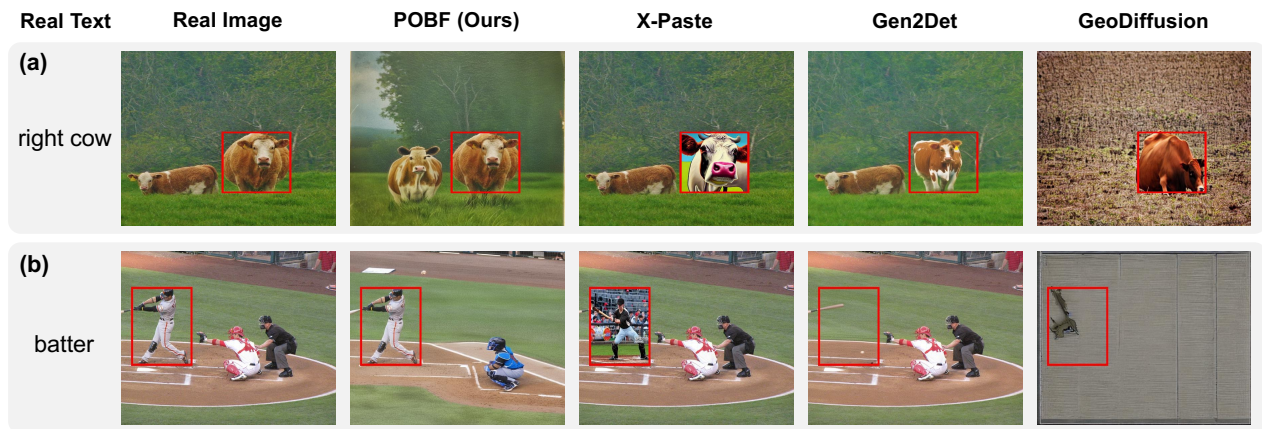


Figure 1: Examples of generated images from different methods. X-Paste [98] synthesizes unnatural images. Gen2Det [63] exhibits the label misalignment issue. GeoDiffusion [5] either fails to generate the correct object or introduces excessive artifacts. In contrast, our method synthesizes high-quality images with accurately aligned bounding boxes.

Abstract

Visual grounding aims to localize the image regions based on a textual query. Given the difficulty of large-scale data curation, we investigate how to effectively learn visual grounding under data-scarce settings in this paper. To address the data scarcity, we propose a novel framework, POBF (Paint Outside the Box and Filter). POBF synthesizes images by inpainting outside the box, tackling a label misalignment issue encountered in previous works. Furthermore, POBF leverages an innovative filtering scheme to select the most effective training data. This scheme combines a hardness score and an overfitting score, balanced by a penalty term. Extensive experiments across four benchmark datasets demonstrate that POBF consistently improves performance, achieving an average gain of 5.83% over the real-data-only method and outperforming leading baselines by 2.29%–3.85% in accuracy. Additionally, we validate the robustness and generalizability of POBF across various generative models, training data sizes, and model architectures.

1 Introduction

Visual grounding [12, 13, 27, 36–38, 40, 58, 73, 89, 94] is a fundamental task in vision-language understanding. The objective is to locate

a specific image region based on a free-form textual query. However, constructing visual grounding datasets with dense region-text annotations is both time-intensive and costly, which hinders the progress in this field. Motivated by the difficulty of large-scale data curation, we investigate the feasibility of effectively learning visual grounding under data-scarce settings, where only few real training data are accessible.

With recent advances in image generation and captioning [32, 39, 50, 51], a natural approach to address data scarcity is to synthesize training data. These powerful generative models, pretrained on large-scale real-world data, have captured the correspondence between images and textual descriptions. It is probable that distilling such knowledge can benefit visual grounding through training data generation. Many recent works [3, 5, 15–17, 35, 81, 98] have explored the generation of densely annotated data to train models for fine-grained understanding tasks, such as object detection and image segmentation. However, they often rely on specialized networks trained on extensive dense annotations, which limits their flexibility and generalizability.

To overcome this limitation, we propose to leverage off-the-shelf generative models, trained solely on image-caption pairs in a weakly-supervised manner, for training data generation. Compared

to the methods relying on specialized networks, our method offers two advantages. First, our method could generalize across a wider range of domains, since the generative models we used are trained on web-scale image-caption data. Second, we can benefit from the rapid progress in generative models, incorporating the latest advancements into our data generation pipeline without additional training on dense annotations.

Although the off-the-shelf generative models are capable of synthesizing images across diverse domains, they struggle to directly generate data with region-text labels, as they are not trained with dense annotations. Therefore, we leverage the limited region-text annotations available in real data to generate training data through inpainting. However, a naive approach—inpainting the object within the bounding box (*e.g.*, Gen2Det [63], see Figure 1)—can result in label misalignment issues. Specifically, the generated object may not spatially align well with the box or even fail to appear entirely. For example, the synthetic ‘right cow’ in Figure 1(a) misaligns with the box, and the ‘batter’ in Figure 1(b) disappears. To tackle the label misalignment problem, we propose a paint-outside-the-box strategy, which preserves the content within the box while generating the background outside. This results in higher-quality images that align well with the original annotations.

Moreover, training neural networks with synthetic data presents another challenge: not all samples contribute positively to the model performance [3, 11, 44, 45]. To identify the most effective training data, we propose a filtering scheme consisting of three components: a hardness score, an overfitting score, and a penalty term. The hardness score prioritizes the easiest samples, as it is challenging to model outliers when the basic patterns are not adequately captured in our data-scarce regime [57]. The overfitting score penalizes samples exacerbating overfitting the unintended features outside the box, as shortcut features from the background could lead the gigantic model to overfit [2, 18, 72], especially with limited training data. Furthermore, to manage the trade-off between two scores, we introduce a penalty term. Finally, we combine the selected synthetic data with the real data to train our visual grounding model.

In summary, we propose a novel framework named POBF (Paint Outside the Box and Filter). POBF synthesizes high-quality training samples by image inpainting and captioning, then employs an effective filtering scheme for data selection. Our contributions are:

- We address a challenging problem of visual grounding in data-scarce scenarios by introducing POBF, a flexible and adaptable framework that leverages off-the-shelf data generators pretrained solely on image-caption pairs.
- We propose a novel data generation strategy for visual grounding, paint outside the box, which overcomes the label misalignment issues in previous approaches.
- We introduce a new filtering scheme designed for data-scarce settings to identify the most effective synthetic training samples. This scheme integrates a hardness score, an overfitting score, and a penalty term.
- Experiments demonstrate that POBF improves performance by 5.83% over real-data-only training and outperforms strong baselines by a 2.29%–3.85% margin. We further validate its robustness and generalizability across generative models, training data sizes, and model architectures.

2 Related Work

Visual Grounding. Early approaches addressed visual grounding in a two-stage framework [38, 40, 91], which heavily depended on the quality of proposals and large computational costs due to the large number of proposals. To overcome the limitations, more efficient one-stage methods have been developed [8, 12, 13, 25, 27, 55, 59, 70, 74, 75, 82, 88, 90]. TransVG [12] incorporates a DETR encoder for visual feature extraction and introduces the first transformer-based framework for visual grounding. QRNet [90], VG-LAW [59], and TransVG++ [13], integrate language-guided knowledge within the intermediate layers of visual backbones to compute query-dependent visual attention dynamically. As the first diffusion-based framework, LG-DVG [9] progressively reasons the queried object by denoising noisy boxes with the language guide.

With the development of pretrained large multimodal models, several studies [19, 20, 28, 80, 85] have leveraged these foundation models to localize objects. For example, [20, 85] employ GradCAM [54] to produce gradient-based visual explanations, represented as heatmaps for grounding outputs. [28] demonstrates that only a few attention heads in large vision-language models can provide accurate and interpretable text-image attention maps for object localization. Inspired by reinforcement learning, ViGoR [80] integrates a reward model for visual grounding outputs, then use the reward model for instruction tuning pretrained multimodal models. In parallel, other works [4, 6, 95, 97] focus on training multimodal large language models for visual grounding using extensive, fine-grained labeled datasets. Furthermore, recent research has expanded traditional visual grounding to gigapixel-level [43] and sensing [62] domain images.

Previous works typically train models on large-scale labeled visual grounding datasets. To mitigate the issue of data scarcity, several studies have explored unsupervised [68], weakly-supervised [10, 26, 41, 42, 61], and semi-supervised [60] learning methods. However, these methods still rely heavily on the availability of large amount of in-domain real data. Instead, we explore a more constrained data-scarce setting, where only a limited amount of real visual grounding data exists. We further propose a data generation strategy and filtering scheme for data-scarce visual grounding.

Training with Synthetic Data. Building off image generation and image captioning, training on synthetic data has emerged as a promising research direction [14, 53, 65, 78, 86]. In fine-grained understanding tasks, researchers explore the use of synthetic data in object detection [5, 16, 17, 63, 69, 96], image segmentation [15, 35, 76, 81, 98], and visual grounding [21, 22, 67]. Some methods [17, 35, 96] incorporate task-specific heads into image generators and fine-tune them with extensive data to synthesize images paired with annotations. Others [15, 21, 98] first generate images, then employ an auxiliary model to annotate the synthetic data. For instance, DiverGen [15] generates images by a vanilla diffusion model and subsequently uses SAM [30] for dense annotation. Several approaches [5, 16, 69, 81] employ visual priors (*e.g.* segmentation masks or edges) to guide the synthetic image generation process via controllable diffusion models. For example, FreeMask [81] uses FreestyleNet [79] to synthesize images conditioned on target dataset-provided masks. However, these methods rely on

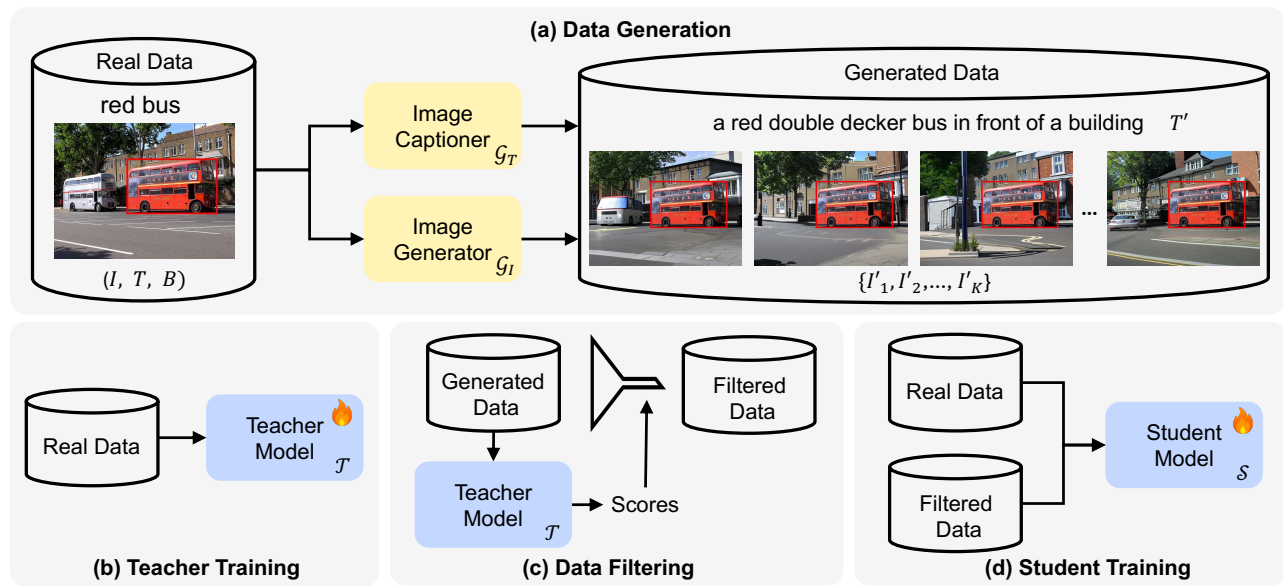


Figure 2: Overview of our proposed framework POBF, which consists of four steps: data generation, teacher training, data filtering, and student training. The real data sample (image, caption, box) is denoted as (I, T, B) . T' and I'_j denote the generated caption and image, respectively. \mathcal{G}_T and \mathcal{G}_I are generative models. \mathcal{T} and \mathcal{S} refer to the teacher and student model, respectively.

either the data generator, the annotator, or both to be pretrained on large-scale densely annotated datasets.

Some prior works [21, 22, 67, 99] have focused on generating labeled training data for visual grounding, but they typically rely on specialized networks—such as object detectors or image generators trained on extensively annotated datasets—which limits their generalizability and flexibility. Departing from these approaches, we introduce a novel training data generation method that leverages off-the-shelf generative models trained solely on image–caption pairs, eliminating the reliance on extensive dense annotations and making our approach more flexible and scalable. In addition, we incorporate a filtering scheme tailored for inpainted images.

Data Pruning. Recent advancements in data selection methods have gained significant attention from the research community [24, 44, 77]. These methods typically employ pre-defined criteria to assign a scalar score to each training example. While simple heuristics like repetition [31], string existence [49], or semantic similarity [1] are commonly used, more sophisticated criteria have also been explored, including gradient norms [48], forgetfulness [66], and influence function scores [83]. A common strategy is to prioritize data samples with lower training loss [7, 87]. This approach leverages the observation that DNNs initially learn generalizable patterns before gradually overfitting to noisy data [34, 56]. To counter confirmation bias, techniques such as co-training models [33, 93] have been proposed, where two networks are trained concurrently and use their combined predictions for selection. MentorNet [23] further extends this idea by introducing a learned curriculum to guide the selection of training data.

Our use of separately trained teacher networks contrasts with recent studies [3, 21, 52, 64, 84] on synthetic training data selection,

which filter out text-image pairs with low CLIP similarity scores. In contrast to prior work, we propose to identify the most effective synthetic training data from the hardness and overfitting perspectives, specifically tailored to the problem of data-scarce visual grounding.

3 Problem Definition

Let I and T denote an input image and a natural language description, respectively. Visual grounding is the task of identifying the target region $R \subseteq I$ within the image that T refers to. Typically, R is represented as a bounding box $B = (x, y, w, h)$, where (x, y) specifies the box center coordinates, and w and h define its width and height. In this paper, we investigate the problem of learning visual grounding in data-scarce scenarios, namely data-scarce visual grounding, where only a very limited amount of annotated real training data is available—e.g., as little as 1% of the dataset.

4 Methodology

To address the data-scarce visual grounding problem, we introduce a novel, model-agnostic framework called POBF (Paint Outside the Box and Filter). As illustrated in Figure 2, POBF consists of four stages. (a) Our approach begins with a data generation process, where we synthesize images and captions using image inpainting and captioning techniques. This process utilizes the image generator and captioner pretrained on large-scale image-caption pairs. (b) Next, we train a teacher model using the limited real data. (c) We then apply a filtering scheme to select effective synthetic images. Specifically, the well-trained teacher network assigns a hardness score, an overfitting score, and a penalty term to each synthetic image. (d) Finally, we retain the synthetic images with high scores and combine them with real data to train the student model. The

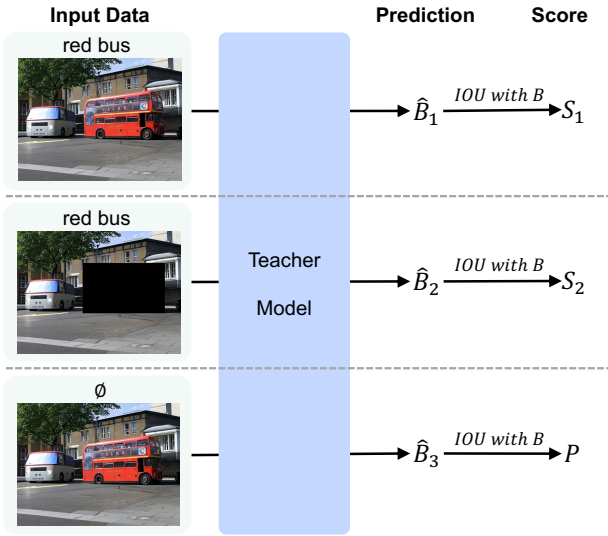


Figure 3: Illustration of the inputs used to compute each score for a generated image. Here, B and \hat{B} denote the ground truth and predicted bounding box, respectively.

proposed POBF framework is simple, effective, and does not rely on any auxiliary models pretrained with dense annotated data.

4.1 Cross-modality Data Generation

Image Generation with Inpainting. We begin by synthesizing images through image inpainting, a process that regenerate masked regions within an image based on a given prompt, while keeping the unmasked areas intact. To address the label misalignment problem, we propose to paint outside of the bounding box instead. For each data point (I, T, B) , we first use a captioning model \mathcal{G}_T to generate a caption C for I . The bounding box B , image I , and caption C are then input into the inpainting model \mathcal{G}_I , yielding an generated image I' . As shown in Figure 2(a), the red bus within the bounding box remains unchanged, making it strictly align with the ground truth bounding box after generation. The synthetic image I' can be paired with the original text T and bounding box B to form a new training sample (I', T, B) . By generating K synthetic images per real sample, denoted as $\{I'_1, I'_2, \dots, I'_K\}$, the training dataset effectively increases in size by a factor of K . A key hyperparameter in the inpainting process is *strength*, which controls the amount of noise added to the base image and, consequently influences the similarity between the generated output and the original image. To encourage data diversity, we set the *strength* parameter to a high value.

Text Generation with Captioning. To augment the original text T , we feed the cropped image within the bounding box B to the captioning model \mathcal{G}_T , which generates a new caption T' describing the object. The generated caption T' can be paired with B and either the real image I or the generated image I' to create a new training sample. In this work, we employ p -sampling to improve diversity.

4.2 Filtering Scheme

Recognizing that not all synthetic samples contribute positively to model performance [3, 11, 44, 45], we propose a novel filtering scheme to select the most effective images for training. Initially, we use the limited real training dataset to train a teacher model \mathcal{T} . Then, \mathcal{T} evaluates synthetic images based on two scores and one penalty term to determine their effectiveness as training samples. We provide an illustration in Figure 3 to demonstrate the input used when calculating each score for a synthetic image. For clarity in the following discussions, we assume a real data sample (I, T, B) and denote the set of images generated from it as $\{I'_1, I'_2, \dots, I'_K\}$.

Hardness Score. We propose to filter harmful synthetic images via computing hardness. Intuitively, in our data-scarce regime, it is difficult to model outliers effectively as fundamental patterns may not be fully captured [57]. Since the model require easiest examples to provide coarse-grained information about the target function, we prioritize synthetic images that are less challenging for the teacher model \mathcal{T} . We define the hardness score for each of the synthetic image I'_j , where $j \in \{1, 2, \dots, K\}$, as follows:

$$S_1(I'_j) = \text{IOU}(\mathcal{T}(I'_j, T), B) \quad (1)$$

where $\mathcal{T}(I'_j, T)$ is the predicted bounding box, and IOU (Intersection over Union) is the ratio of the intersection of two areas to their combined area.

Overfitting Score. Additionally, we introduce another score to filter out synthetic images that may hinder training by exacerbating overfitting. Given the gigantic model architecture relative to the limited number of real data, the model is prone to overfit by relying on image background features rather than the actual object in the bounding box [2, 72]. To mitigate this, we assess the potential of each generated image to contribute to overfitting. Specifically, we modify each generated image by masking the area within the bounding box and input this variant into \mathcal{T} . If \mathcal{T} can still correctly predict the bounding box, it indicates that \mathcal{T} may leverage unintended features present in the generated background. Incorporating such data into training dataset risks the model learning these unintended features, thereby exacerbating overfitting. We define an overfitting score to filter these problematic samples. The score for each generate image I'_j , where $j \in \{1, 2, \dots, K\}$, is defined as:

$$S_2(I'_j) = 1 - \text{IOU}(\mathcal{T}(\text{Mask}(I'_j, B), T), B) \quad (2)$$

where $\text{Mask}(I'_j, B)$ is a operation that sets all pixel values within the bounding box B to zero.

Penalty Term. To balance between preserving easy samples and the mitigation of overfitting risk, we introduce a penalty term. The rationale is that overly easy images may not challenge the model enough to learn complex patterns. Conversely, images where the background outside the bounding box does not offer any useful information may introduce model bias. To balance between the first two scores, we define a penalty term for each generate image I'_j , where $j \in \{1, 2, \dots, K\}$, as follows:

$$P(I'_j) = \text{IOU}(\mathcal{T}(I'_j, \emptyset), B) \quad (3)$$

where \emptyset denote an empty textual string. This term can be regarded as the prior knowledge in the generated image.

The three scores are individually normalized to have zero mean and unit standard deviation. Then The final score for a generated image I'_j is calculated as:

$$\text{Score}(I'_j) = \lambda_1 S_1(I'_j) + \lambda_2 S_2(I'_j) + \lambda_P P(I'_j) \quad (4)$$

where λ_1 , λ_2 , and λ_P are hyperparameters controlling the weights of each component.

Out of the K generated images $\{I'_1, I'_2, \dots, I'_K\}$ from each real data point (I, T, B) , we retain one synthetic image I'_m with the highest score, where $m = \arg \max_j \text{Score}(I'_j)$ and $j \in \{1, 2, \dots, K\}$. This yields a synthetic data point (I', T, B) . By incorporating the selected synthetic data points into the training set, we effectively double its size. Finally, we train a student model S , where the real text T is randomly replaced with the corresponding generated caption T' with probability q during training.

5 Experiments

Dataset. RefCOCO [92], RefCOCO+ [92], and RefCOCOg [46, 47] datasets are derived from MSCOCO 2014. Following the common splits used in previous studies [12, 13], we report performance on the testA (containing multiple people) and the testB (containing multiple instances of other objects) for RefCOCO and RefCOCO+, and the umd-test splits for RefCOCOg [47]. The ReferItGame dataset [29] is collected through an online two-player game. We report performance on the test set of ReferItGame. The statistics for these four datasets are presented in Table 1. For each dataset, we randomly sample subsets comprising 1% of the entire dataset to simulate data-scarce scenarios.

Table 1: Statistics of visual grounding datasets.

Dataset	Images	Texts	Objects
RefCOCO [92]	19,994	142,210	50,000
RefCOCO+ [92]	19,992	141,564	49,856
RefCOCOg [46, 47]	25,799	95,010	49,822
ReferItGame [29]	19,894	130,525	96,654

Baselines. We compare our method with three state-of-the-art baselines, all of which generate dense annotated training data. (i) X-Paste [98] uses an ensemble of pretrained segmentation models to identify instances from generated images, which are then copied into real images. (ii) Gen2Det [63] employs a grounded editing diffusion model to edit objects in real images. (iii) GeoDiffusion [5] utilizes geometric control via text prompts to enhance text-to-image diffusion models for direct object detection data generation. For a fair comparison, we refrain from using the models that have been pretrained on a large-scale dense annotations. Implementation details can be found in the supplementary material.

Evaluation Metric. Following previous works [12, 13], we use top-1 accuracy as the evaluation metric, where a prediction is considered correct if the IoU between the predicted bounding box and the ground-truth exceeds 0.5.

Implementation Details. For both the teacher and student networks, we utilize TransVG [12], one of the most popular models for visual grounding without any bells or whistles. We utilize the Stable

Diffusion XL model [50] for image inpainting, with 45 denoising steps, a strength of 0.9, and a guidance scale of 7.5. BLIP ViT-L [32] is employed as the image captioner, with nucleus sampling ($p=0.9$). The hyperparameters λ in filtering scheme is tuned using grid search on the validation set, with values of 1.0 or 0.5. For each real data point, we generate 4 synthetic images and retain one with highest score. During training, generated texts replace real captions with a probability of $q = 0.3$. For a fair comparison, we adopt a consistent training schedule (batch size \times steps = 64×6500) across all experiments, following [69, 81, 96].

5.1 Main Results

Comparison with State-of-the-Art Baselines. We have following observations from Table 2. **(1) Synthetic data provides substantial performance gains.** Models utilizing synthetic data generated by various baselines consistently outperform the method trained solely on real data, with at least a 1.98% improvement. This demonstrates the strong potential of synthetic data in boosting model performance. Our approach further improves upon this, achieving an average performance gain of 5.83% over the real-data-only baseline, which highlights the effectiveness of our generation strategy. **(2) POBF outperforms the baseline that directly generates training data by a significant margin.** GeoDiffusion is capable of directly generating images from scratch. However, it fails to correctly generate an image for batter in Figure 1. This is because fine-tuning over a fixed set of objects within a specific domain limits its generalizability to novel targets. Consequently, our method surpasses GeoDiffusion by an average margin of 3.85%. **(3) POBF consistently outperforms image editing baselines.** Similar to POBF, both Gen2Det and X-Paste generate training samples by editing real images. The strongest baseline, X-Paste, achieves an average score of 31.32%, while our method exceeds this by 2.29%. In Figure 1, X-Paste produces unnatural images, and Gen2Det suffers from label misalignment issues. These quality limitations hinder model performance. In contrast, POBF generates high-quality, natural images with accurately aligned bounding boxes. In addition, we hypothesize that the relatively modest improvement on ReferIt stems from the small objects in this dataset. The inpainting process requires generating very large background regions, which may introduce visible artifacts that hinder model performance. In conclusion, our method establishes a new benchmark for visual grounding in data-scarce scenarios.

Average Results on Three Randomly Sampled Datasets. Additionally, we sampled three different subsets from each dataset to further evaluate performance in Table 2. While there is some performance variance due to the relatively small size of the sampled datasets, our method consistently outperforms the model trained solely on real data across four datasets. These results highlight the robustness of our approach to varying data distributions.

5.2 Ablation Study

Ablation on Synthetic Data. We begin by evaluating the effectiveness of synthetic data by separately using generated images and texts, without the filtering scheme. We observe that using only real data results in relatively low performance, with the model achieving

Table 2: Performance comparison with state-of-the-art baselines. All methods employ the proposed filtering scheme.

Method	Dataset		RefCOCO		RefCOCO+		RefCOCog	ReferIt	Avg
	Real	Syn	TestA	TestB	TestA	TestB	Test	Test	
<i>Results on One Sampled Dataset</i>									
Real	✓		44.26	34.34	23.58	17.70	24.87	21.87	27.78
GeoDiffusion [5]	✓	✓	47.22	34.90	28.01	18.83	25.39	24.20	29.76 ^{+1.98}
Gen2Det [63]	✓	✓	46.61	35.19	<u>28.85</u>	<u>20.65</u>	26.10	25.00	30.40 ^{+2.62}
X-Paste [98]	✓	✓	<u>47.85</u>	<u>39.01</u>	27.59	21.25	<u>27.08</u>	<u>25.16</u>	<u>31.32</u> ^{+3.54}
POBF (Ours)	✓	✓	52.77	40.96	31.37	21.25	29.98	25.28	33.61 ^{+5.83}
<i>Average Results across Three Sampled Datasets</i>									
Real	✓		43.64 ^{±0.98}	34.89 ^{±0.50}	25.15 ^{±1.43}	18.02 ^{±1.48}	24.92 ^{±1.05}	22.94 ^{±0.97}	28.26
POBF (Ours)	✓	✓	51.25 ^{±1.49}	39.62 ^{±1.16}	32.15 ^{±0.68}	22.38 ^{±1.01}	30.73 ^{±0.69}	25.10 ^{±0.30}	33.54 ^{+5.28}

Table 3: Ablations on the synthetic data and filtering scheme. Syn_{img} and Syn_{txt} denote synthetic images and texts, respectively.

Training Data			Filtering			RefCOCO		RefCOCO+		RefCOCog	ReferIt	Avg
Real	Syn_{img}	Syn_{txt}	S_1	S_2	P	TestA	TestB	TestA	TestB	Test	Test	
<i>the Effectiveness of the Synthetic Data</i>												
✓						44.26	34.34	23.58	17.70	24.87	21.87	27.78
✓	✓					49.97	39.16	29.01	20.56	26.67	22.49	31.31 ^{+3.53}
✓		✓				47.00	36.19	25.36	18.74	26.33	22.13	29.29 ^{+1.51}
<i>the Effectiveness of the Filtering Scheme</i>												
✓	✓	✓				50.13	38.86	29.10	20.10	28.31	23.39	31.65 ^{+3.87}
✓	✓	✓	✓			50.66	39.56	30.63	<u>21.76</u>	30.18	24.50	32.88 ^{+5.10}
✓	✓	✓		✓		50.29	39.67	29.95	21.17	28.42	24.67	32.36 ^{+4.58}
✓	✓	✓			✓	51.15	39.24	30.22	21.44	29.70	<u>25.01</u>	32.79 ^{+5.01}
✓	✓	✓	✓	✓		<u>51.94</u>	<u>39.75</u>	<u>30.65</u>	22.44	29.41	24.30	33.08 ^{+5.30}
✓	✓	✓	✓	✓	✓	52.77	40.96	31.37	21.25	<u>29.98</u>	25.28	33.61 ^{+5.83}

an average accuracy of 27.78%. Introducing synthetic images leads to a significant improvement, boosting performance by 3.53% on average, demonstrating the effectiveness of our proposed inpainting strategy. When synthetic texts are applied, the improvement is modest at 1.51%, demonstrating the importance of generated texts for performance gains.

Ablation on Filtering Scheme. Next, we assess the effectiveness of different components of our filtering scheme. The individual components— S_1 , S_2 , and P —result in performance gains of 1.23%, 0.71%, and 1.14%, respectively, compared to the variant without any filtering. These results demonstrate the effectiveness of each component in selecting valuable training data. Notably, the variant excludes only the penalty term achieves an accuracy of 33.08%, surpassing all configurations that utilize a single filtering component. The full filtering scheme yields the highest accuracy across all datasets, reaching an average accuracy of 33.61%. This represents a substantial improvement of 1.96% over the baseline without filtering, further underscoring the effectiveness of our proposed filter scheme. In conclusion, both synthetic data and filtering schemes play crucial roles in enhancing model performance, with the combination of these elements yielding the best results.

5.3 Filtering Scheme Analysis

We isolate the each component in the filtering scheme, excluding the influence of generated text, offering insights into their impact on model performance. Inspired by recent advances in data selection [3, 21, 52, 57, 64, 71, 84], we construct several adapted baselines by modifying these methods to fit within our teacher-based data selection framework. (i) *Random teacher*: randomly selects synthetic images as training data. (ii) *No teacher*: uses all synthetic data indiscriminately for training. (iii) *CLIP teacher*: a commonly used approach in prior works [3, 21, 52, 64, 84], which selects synthetic images with the highest cosine similarity with the real text. (iv) *Moderate-Loss* [71]: defines the score as the difference between a sample’s loss and the class mean loss, prioritizing samples with scores near the median. (v) *Moderate-DS* [71]: replaces the score in *Moderate-Loss* with the Euclidean distance between a sample’s embedding and the class center embedding, again favoring samples near the median. (vi) *Difficult-Loss* [57]: prioritizes hard examples with higher loss values. In addition, we include two variants of our method that select training samples based on the negative hardness score ($-S_1$) and negative overfitting score ($-S_2$), respectively.

We have following observations in Table 4. **(1) Simply increasing the amount of synthetic data does guarantee improved**

Table 4: Results obtained by isolating scores without generated text. Results with a gray background indicate performance lower than the *Random teacher* baseline.

Filter	RefCOCO		RefCOCO+		Avg
	TestA	TestB	TestA	TestB	
Random teacher	48.52	38.84	27.47	20.27	33.76
No teacher	48.45	38.68	28.40	20.29	33.96 ^{+0.20}
CLIP teacher [3]	48.84	39.75	28.07	20.35	34.25 ^{+0.49}
Moderate-Loss [71]	48.86	39.17	27.01	21.17	34.05 ^{+0.29}
Moderate-DS [71]	49.61	40.47	28.21	19.84	34.31 ^{+0.55}
Difficult-Loss [57]	46.95	37.03	27.73	19.45	32.97 ^{-0.79}
<i>Our Proposed Filtering Scheme</i>					
- S_1	48.17	38.90	25.98	19.25	33.38 ^{-0.38}
- S_2	48.22	38.51	26.86	19.60	33.30 ^{-0.46}
S_1	49.94	40.14	29.53	20.67	35.07 ^{+1.31}
S_2	49.48	39.83	27.68	20.35	34.34 ^{+0.58}
P	50.66	39.47	28.50	20.41	34.67 ^{+0.91}
S_1+S_2+P	50.98	40.53	30.25	20.51	35.56^{+1.81}

performance. Although the *No teacher* method utilizes more data than the *Random teacher* baseline, it sometimes yields inferior results. For example, it shows performance drops of 0.07% and 0.16% on RefCOCO. It underscores the importance of filtering out low-quality data to ensure the effectiveness of the training data. **(2) Incorporating any individual score from our filtering scheme leads to significant performance improvements over all baselines.** The three methods with any individual score outperform all baselines with gains ranging from 0.58% to 1.31%. Notably, they also surpasses the *CLIP teacher* baseline, which is commonly used for synthetic data selection. This demonstrates the effectiveness of filtering based on hardness and overfitting perspectives compared to CLIP similarity. The observation of their effectiveness aligns with our observations in Table 3, when synthetic texts are incorporated. **(3) Combining all three scores yields the best overall performance.** Our full filtering scheme, which integrates all three components, outperforms all baselines with improvements ranging from 1.26% to 2.60%. In particular, it exceeds the *CLIP teacher* baseline by 1.32% on average. This result underscores the complementary nature of the three scores and their ability to be seamlessly integrated for enhanced performance. **(4) Interestingly, filtering based on negative values of S_1 or S_2 results in worse performance than the *Random teacher* baseline.** For example, applying $-S_1$ and $-S_2$ leads to average performance drops of 0.38% and 0.46% across the two datasets. The observed performance declines when using negative scores suggests that our filtering scheme is effective in identifying valuable training data, as the introduction of poorly selected data (as indicated by negative scores) degrades model performance.

Relationship between 2 Scores. We visualize the relationship between the hardness score S_1 and the overfitting score S_2 on the (a) RefCOCO and (b) RefCOCog datasets in Figure 4. As shown, there is a weak negative correlation between the two scores. The absence of a strong linear relationship between the two scores suggests that S_1 and S_2 capture different aspects of data quality, offering

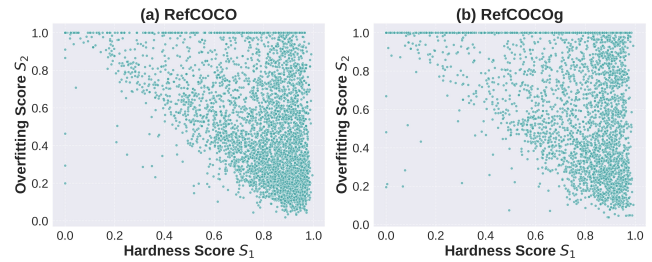


Figure 4: Scatter plot illustrating the relationship between unnormalized hardness score S_1 and overfitting score S_2 across different datasets. Each point presents a generated sample.

Table 5: Performance comparison across generative models.

Method	RefCOCO+		RefCOCog	Avg
	TestA	TestB	Test	
Real	23.58	17.70	23.95	21.74
POBF (Ours)	31.37	21.25	<u>29.98</u>	<u>27.53^{+5.79}</u>
<i>Replace the Image Captioner with . . .</i>				
LLAVA [39]	31.09	<u>21.54</u>	28.57	27.07 ^{+5.33}
ViT-GPT2 ²	29.95	21.22	29.90	27.02 ^{+5.28}
<i>Replace the Image Generator with . . .</i>				
SD 2 [51]	<u>31.16</u>	21.19	29.30	27.22 ^{+5.48}
Dreamshaper ¹	30.20	22.39	30.32	27.63^{+5.89}

complementary perspectives when selecting effective training samples. To further quantify this relationship, we compute the Pearson correlation coefficients for the two datasets, which are -0.4589 for RefCOCO and -0.3810 for RefCOCog, respectively. These moderate correlation values highlight their potential in jointly guiding data selection.

5.4 Cross-modality Generative Models

We evaluate whether POBF can seamlessly integrate with other state-of-the-art pretrained generative models. By default, POBF utilizes Stable Diffusion XL [50] as the image generator and BLIP ViT-L [32] as the image captioner. In this experiment, we test two alternative image generators: Stable Diffusion 2 [51] and Dreamshaper¹. For image captioning, we explore replacements such as LLAVA [39] and ViT-GPT2². Table 5 shows the results. We observe that while the default configuration of POBF demonstrates strong performance, it does not always yield the highest accuracy. Specifically, model combinations using Dreamshaper as the image generator achieve superior outcomes, reaching an average accuracy of 27.63%. Furthermore, these configurations consistently outperform the baseline, which highlights the generalizability and effectiveness of our proposed framework.

¹<https://huggingface.co/Lykon/dreamshaper-8-inpainting>

²<https://huggingface.co/nlpconnect/vit-gpt2-image-captioning>

Table 6: Performance comparison across training data sizes.

Method	RefCOCO+		RefCOCOg	Avg
	TestA	TestB	Test	
<i>0.5% Training Data</i>				
Real	16.42	10.07	15.43	13.97
POBF (Ours)	21.41	15.87	20.28	19.18+5.22
<i>2.0% Training Data</i>				
Real	33.04	25.03	33.28	30.45
POBF (Ours)	37.68	29.88	38.97	35.51+5.06

Table 7: Performance comparison across model architectures. #Paras denotes the number of trainable model parameters.

Method	RefCOCO+		RefCOCOg	Avg
	TestA	TestB	Test	
<i>TransVG [12] (#Paras = 149M)</i>				
Real	23.58	17.70	23.95	21.74
POBF (Ours)	31.37	21.25	29.98	27.53+5.79
<i>Dynamic-MDTRE [55] (#Paras = 160M)</i>				
Real	23.82	18.55	29.07	23.81
POBF (Ours)	33.55	23.93	35.03	30.84+7.03
<i>QRNet [90] (#Paras = 273M)</i>				
Real	32.32	23.82	30.30	28.81
POBF (Ours)	37.29	26.65	35.73	33.22+4.41

5.5 Training Data Sizes

Table 6 presents the performance of our proposed framework under varying amounts of training data. We evaluate two scenarios: using 0.5% and 2.0% of the original training set, and report the average accuracy over three randomly sampled datasets per setting. With only 0.5% of the data, the real-data-only baseline achieves 13.97% accuracy, while our method improves this to 19.18%, yielding a substantial gain of 5.22%. At 2.0% data, our framework further increases accuracy by 5.06%. These consistent improvements highlight the robustness and effectiveness of our approach in data-scarce environments, demonstrating its potential for real-world applications where labeled data is limited.

5.6 Model Architectures

We evaluate the proposed POBF framework across different model architectures to assess its generalizability and effectiveness. Specifically, we experiment with TransVG [12], Dynamic-MDTRE [55], and QRNet [90], each of which differs in terms of the number of parameters and architectural complexity. Table 7 presents the results. Although model performance generally increases with model size, our POBF framework yields substantial improvements across all tested architectures. Notably, Dynamic-MDTRE shows the largest gain, with a 7.03% increase in average accuracy. QRNet, the most complex model with 273M parameters, also benefits from a 4.41% improvement. The results highlight that our method is not tailored to a specific architecture but instead offers consistent performance benefits across diverse model designs.

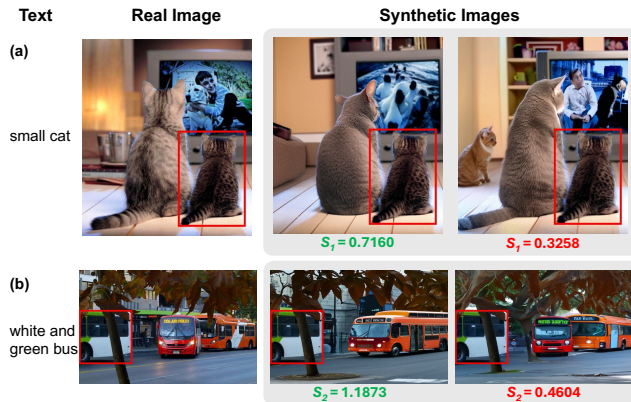


Figure 5: Qualitative examples illustrating the effectiveness of the two proposed scores. The green score indicates the synthetic image with the higher corresponding score.

5.7 Case Study

Generative models may occasionally produce ambiguous examples that degrade model performance. They can also generate synthetic images that closely resemble real ones, increasing the risk of overfitting. In Figure 5, we present two representative examples illustrating how the hardness score (S_1) and the overfitting score (S_2) help to mitigate these two issues and select the effective data.

In Figure 5(a), the second synthetic image contains a small cat in the background, which may confuse the model when attempting to localize the target object `small cat`. Since this example is difficult for the teacher model to localize correctly, it receives a low S_1 and could thus be filtered out.

In Figure 5(b), the background of the second generated image is visually very similar to the real image — the color, position, and posture of the two buses closely resembles those in the real image. Including such a similar sample in training data may significantly increase the risk of overfitting. In contrast, the first generated image background presents a bus with a noticeably different appearance and placement compared to the real image. As a result, the teacher model assigns a higher S_2 to the first image, indicating it is less likely to induce overfitting and is more suitable for training.

6 Conclusions

In this paper, we introduced POBF, a novel framework for effectively learning visual grounding in data-scarce scenarios. Leveraging advanced generative models pretrained solely on image-caption pairs, POBF enables high-quality synthetic data generation. By avoiding reliance on specialized networks trained on extensive dense annotations, POBF gains enhanced flexibility and generalizability. Specifically, we proposed a new data generation strategy—paint outside the box—which addresses the label misalignment issues commonly encountered in previous approaches. Additionally, to select the most effective synthetic samples, we introduced a novel filtering scheme tailored for inpainted data. This scheme integrates a hardness score, an overfitting score, and a penalty term. Experimental results demonstrate that POBF achieves an average improvement

of 5.83% over the real-data-only baseline across four benchmark datasets. It also surpasses leading baselines, with accuracy gains ranging from 2.74% to 4.35%. Ablation studies confirm that our data generation strategy and filtering scheme contribute significant improvements of 3.53% and 1.96%, respectively. We further validated the robustness and generalizability of POBF across different generative models, training data sizes, and model architectures, and illustrated the effectiveness of our filtering scheme through detailed case analysis. Overall, we believe our approach offers valuable insights and opens new avenues for future research in training data generation and data selection from new perspectives.

References

- [1] Amro Abbas, Kushal Tirumala, Dániel Simig, Surya Ganguli, and Ari S Morcos. 2023. Semdedup: Data-efficient learning at web-scale through semantic deduplication. *arXiv preprint arXiv:2303.09540* (2023).
- [2] Sara Beery, Grant Van Horn, and Pietro Perona. 2018. Recognition in terra incognita. In *Proceedings of the ECCV*. 456–473.
- [3] Fangyi Chen, Han Zhang, Zhantao Yang, Hao Chen, Kai Hu, and Marios Savvides. 2024. RTGen: Generating Region-Text Pairs for Open-Vocabulary Object Detection. *arXiv preprint arXiv:2405.19854* (2024).
- [4] Gongwei Chen, Leyang Shen, Rui Shao, Xiang Deng, and Liqiang Nie. 2024. Lion: Empowering multimodal large language model with dual-level visual knowledge. In *Proceedings of the IEEE/CVF CVPR*. 26540–26550.
- [5] Kai Chen, Enze Xie, Zhe Chen, Yibo Wang, HONG Lanqing, Zhenguo Li, and Dit-Yan Yeung. 2024. GeoDiffusion: Text-Prompted Geometric Control for Object Detection Data Generation. In *The Twelfth International Conference on Learning Representations*.
- [6] Keqin Chen, Zhao Zhang, Weili Zeng, Richong Zhang, Feng Zhu, and Rui Zhao. 2023. Shikra: Unleashing multimodal llm’s referential dialogue magic. *arXiv preprint arXiv:2306.15195* (2023).
- [7] Pengfei Chen, Ben Ben Liao, Guangyong Chen, and Shengyu Zhang. 2019. Understanding and utilizing deep neural networks trained with noisy labels. In *International Conference on Machine Learning*. PMLR, 1062–1070.
- [8] Sijia Chen and Baochun Li. 2022. Multi-modal dynamic graph transformer for visual grounding. In *Proceedings of the IEEE/CVF CVPR*. 15534–15543.
- [9] Sijia Chen and Baochun Li. 2023. Language-guided diffusion model for visual grounding. *arXiv preprint arXiv:2308.09599* (2023).
- [10] Shengxin Chen, Gen Luo, Yiyi Zhou, Xiaoshuai Sun, Guannan Jiang, and Rongrong Ji. 2024. QueryMatch: A Query-based Contrastive Learning Framework for Weakly Supervised Visual Grounding. In *Proceedings of the 32nd ACM International Conference on Multimedia*. 4177–4186.
- [11] Yicheng Chen, Xiangtai Li, Yining Li, Yanhong Zeng, Jianzong Wu, Xiangyu Zhao, and Kai Chen. 2024. Auto Cherry-Picker: Learning from High-quality Generative Data Driven by Language. *arXiv preprint arXiv:2406.20085* (2024).
- [12] Jiajun Deng, Zhengyuan Yang, Tianlang Chen, Wengang Zhou, and Houqiang Li. 2021. Transvg: End-to-end visual grounding with transformers. In *Proceedings of the IEEE/CVF ICCV*. 1769–1779.
- [13] Jiajun Deng, Zhengyuan Yang, Daqing Liu, Tianlang Chen, Wengang Zhou, Yanyong Zhang, Houqiang Li, and Wanli Ouyang. 2023. Transvg++: End-to-end visual grounding with language conditioned vision transformer. *IEEE transactions on pattern analysis and machine intelligence* (2023).
- [14] Zilin Du, Yunxin Li, Xu Guo, Yidan Sun, and Boyang Li. 2023. Training Multimedia Event Extraction With Generated Images and Captions. *arXiv preprint arXiv:2306.08966* (2023).
- [15] Chengxiang Fan, Muzhi Zhu, Hao Chen, Yang Liu, Weijia Wu, Huaqi Zhang, and Chunhua Shen. 2024. DiverGen: Improving Instance Segmentation by Learning Wider Data Distribution with More Diverse Generative Data. In *Proceedings of the IEEE/CVF CVPR*. 3986–3995.
- [16] Haoyang Fang, Boran Han, Shuai Zhang, Su Zhou, Cuixiong Hu, and Wen-Ming Ye. 2024. Data augmentation for object detection via controllable diffusion models. In *Proceedings of the IEEE/CVF WACV*. 1257–1266.
- [17] Chengjian Feng, Yujie Zhong, Zequn Jie, Weidi Xie, and Lin Ma. 2024. Instagen: Enhancing object detection by training on synthetic dataset. In *Proceedings of the IEEE/CVF CVPR*. 14121–14130.
- [18] Robert Geirhos, Jörn-Henrik Jacobsen, Claudio Michaelis, Richard Zemel, Wieland Brendel, Matthias Bethge, and Felix A Wichmann. 2020. Shortcut learning in deep neural networks. *Nature Machine Intelligence* 2, 11 (2020).
- [19] Zeyu Han, Fangrui Zhu, Qianru Lao, and Huaizu Jiang. 2024. Zero-shot referring expression comprehension via structural similarity between images and captions. In *Proceedings of the IEEE/CVF CVPR*. 14364–14374.
- [20] Ruozhen He, Paola Cascante-Bonilla, Ziyang Yang, Alexander C Berg, and Vicente Ordonez. 2024. Improved Visual Grounding through Self-Consistent Explanations. In *Proceedings of the IEEE/CVF CVPR*. 13095–13105.
- [21] Ruozhen He, Paola Cascante-Bonilla, Ziyang Yang, Alexander C Berg, and Vicente Ordonez. 2024. Learning from Models and Data for Visual Grounding. *arXiv preprint arXiv:2403.13804* (2024).
- [22] Haojun Jiang, Yuanze Lin, Dongchen Han, Shiji Song, and Gao Huang. 2022. Pseudo-q: Generating pseudo language queries for visual grounding. In *Proceedings of the IEEE/CVF CVPR*.
- [23] Lu Jiang, Zhengyuan Zhou, Thomas Leung, Li-Jia Li, and Li Fei-Fei. 2018. Mentor-net: Learning data-driven curriculum for very deep neural networks on corrupted labels. In *International conference on machine learning*. PMLR.
- [24] Yiding Jiang, Allan Zhou, Zhili Feng, Sadhika Malladi, and J Zico Kolter. 2024. Adaptive Data Optimization: Dynamic Sample Selection with Scaling Laws. *arXiv preprint arXiv:2410.11820* (2024).
- [25] Yang Jiao, Zequn Jie, Jingjing Chen, Lin Ma, and Yu-Gang Jiang. 2023. Suspected Objects Matter: Rethinking Model’s Prediction for One-stage Visual Grounding. In *Proceedings of the 31st ACM International Conference on Multimedia*. 17–26.
- [26] Lei Jin, Gen Luo, Yiyi Zhou, Xiaoshuai Sun, Guannan Jiang, Annan Shu, and Rongrong Ji. 2023. Refclip: A universal teacher for weakly supervised referring expression comprehension. In *Proceedings of the IEEE/CVF CVPR*. 2681–2690.
- [27] Aishwarya Kamath, Mannat Singh, Yann LeCun, Gabriel Synnaeve, Ishan Misra, and Nicolas Carion. 2021. Mdetr-modulated detection for end-to-end multi-modal understanding. In *Proceedings of the IEEE/CVF ICCV*. 1780–1790.
- [28] Seil Kang, Jinyeong Kim, Junhyeok Kim, and Seong Jae Hwang. 2025. Your Large Vision-Language Model Only Needs A Few Attention Heads For Visual Grounding. *arXiv preprint arXiv:2503.06287* (2025).
- [29] Sahar Kazemzadeh, Vicente Ordonez, Mark Matten, and Tamara Berg. 2014. Referitgame: Referring to objects in photographs of natural scenes. In *Proceedings of the 2014 conference on EMNLP*. 787–798.
- [30] Alexander Kirillov, Eric Mintun, Nikhila Ravi, Hanzi Mao, Chloe Rolland, Laura Gustafson, Tete Xiao, Spencer Whitehead, Alexander C Berg, Wan-Yen Lo, et al. 2023. Segment anything. In *Proceedings of the IEEE/CVF ICCV*. 4015–4026.
- [31] Katherine Lee, Daphne Ippolito, Andrew Nystrom, Chiyuan Zhang, Douglas Eck, Chris Callison-Burch, and Nicholas Carlini. 2021. Duplicating training data makes language models better. *arXiv preprint arXiv:2107.06499* (2021).
- [32] Junnan Li, Dongxu Li, Caiming Xiong, and Steven Hoi. 2022. Blip: Bootstrapping language-image pre-training for unified vision-language understanding and generation. In *International conference on machine learning*. PMLR, 12888–12900.
- [33] Junnan Li, Richard Socher, and Steven CH Hoi. 2020. Dividemix: Learning with noisy labels as semi-supervised learning. *arXiv preprint arXiv:2002.07394* (2020).
- [34] Mingchen Li, Mahdi Soltanolkotabi, and Samet Oymak. 2020. Gradient descent with early stopping is provably robust to label noise for overparameterized neural networks. In *International conference on artificial intelligence and statistics*. 4313.
- [35] Ziyi Li, Qinye Zhou, Xiaoyun Zhang, Ya Zhang, Yanfeng Wang, and Weidi Xie. 2023. Open-vocabulary object segmentation with diffusion models. In *Proceedings of the IEEE/CVF ICCV*. 7667.
- [36] Yaoyuan Liang, Zhao Yang, Yansong Tang, Jiahuo Fan, Ziran Li, Jingang Wang, Philip HS Torr, and Shao-Lun Huang. 2023. Luna: Language as continuing anchors for referring expression comprehension. In *Proceedings of the 31st ACM International Conference on Multimedia*. 5174–5184.
- [37] Pengyue Lin, Ruifan Li, Yuzhe Ji, Zhihan Yu, Fangxiang Feng, Zhanyu Ma, and Xiaojie Wang. 2024. Triple Alignment Strategies for Zero-shot Phrase Grounding under Weak Supervision. In *Proceedings of the 32nd ACM International Conference on Multimedia*. 4312–4321.
- [38] Daqing Liu, Hanwang Zhang, Feng Wu, and Zheng-Jun Zha. 2019. Learning to assemble neural module tree networks for visual grounding. In *Proceedings of the IEEE/CVF ICCV*. 4673–4682.
- [39] Haotian Liu, Chunyuan Li, Qingyang Wu, and Yong Jae Lee. 2024. Visual instruction tuning. *Advances in neural information processing systems* 36 (2024).
- [40] Xihui Liu, Zihao Wang, Jing Shao, Xiaogang Wang, and Hongsheng Li. 2019. Improving referring expression grounding with cross-modal attention-guided erasing. In *Proceedings of the IEEE/CVF CVPR*. 1950–1959.
- [41] Yongfei Liu, Bo Wan, Lin Ma, and Xuming He. 2021. Relation-aware instance refinement for weakly supervised visual grounding. In *Proceedings of the IEEE/CVF CVPR*. 5612–5621.
- [42] Yang Liu, Jiahua Zhang, Qingchao Chen, and Yuxin Peng. 2023. Confidence-aware pseudo-label learning for weakly supervised visual grounding. In *Proceedings of the IEEE/CVF ICCV*. 2828–2838.
- [43] Tao Ma, Bing Bai, Haozhe Lin, Heyuan Wang, Yu Wang, Lin Luo, and Lu Fang. 2024. When visual grounding meets gigapixel-level large-scale scenes: benchmark and approach. In *Proceedings of the IEEE/CVF CVPR*. 22119–22128.
- [44] Anas Mahmoud, Mostafa Elhoushi, Amro Abbas, Yu Yang, Newsha Ardalani, Hugh Leather, and Ari S Morcos. 2024. Sieve: Multimodal dataset pruning using image captioning models. In *Proceedings of the IEEE/CVF CVPR*. 22423–22432.
- [45] Eran Malach and Shai Shalev-Shwartz. 2017. Decoupling “when to update” from “how to update”. *Advances in neural information processing systems* 30 (2017).
- [46] Junhua Mao, Jonathan Huang, Alexander Toshev, Oana Camburu, Alan L Yuille, and Kevin Murphy. 2016. Generation and comprehension of unambiguous object descriptions. In *Proceedings of the IEEE CVPR*. 11–20.

- [47] Varun K Nagaraja, Vlad I Morariu, and Larry S Davis. 2016. Modeling context between objects for referring expression understanding. In *Computer Vision–ECCV 2016: 14th European Conference*. Springer, 792–807.
- [48] Mansheej Paul, Surya Ganguli, and Gintare Karolina Dziugaite. 2021. Deep learning on a data diet: Finding important examples early in training. *Advances in neural information processing systems* 34 (2021), 20596–20607.
- [49] Guilherme Penedo, Quentin Malartic, Daniel Hesslow, Ruxandra Cojocaru, Alessandro Cappelli, Hamza Alobeidli, Baptiste Pannier, Ebtesam Almazrouei, and Julien Launay. 2023. The RefinedWeb dataset for Falcon LLM: outperforming curated corpora with web data, and web data only. *arXiv preprint arXiv:2306.01116* (2023).
- [50] Dustin Podell, Zion English, Kyle Lacey, Andreas Blattmann, Tim Dockhorn, Jonas Müller, Joe Penna, and Robin Rombach. 2023. Sdxl: Improving latent diffusion models for high-resolution image synthesis. *arXiv preprint arXiv:2307.01952* (2023).
- [51] Robin Rombach, Andreas Blattmann, Dominik Lorenz, Patrick Esser, and Björn Ommer. 2022. High-resolution image synthesis with latent diffusion models. In *Proceedings of the IEEE/CVF CVPR*. 10684–10695.
- [52] Daniel Rose, Vaishnavi Himakunthala, Andy Ouyang, Ryan He, Alex Mei, Yujie Lu, Michael Saxon, Chinmay Sonar, Diba Mirza, and William Yang Wang. 2023. Visual Chain of Thought: Bridging Logical Gaps with Multimodal Infillings. *arXiv preprint arXiv:2305.02317* (2023).
- [53] Noam Rotstein, David Bensaïd, Shaked Brody, Roy Ganz, and Ron Kimmel. 2024. Fusecap: Leveraging large language models for enriched fused image captions. In *Proceedings of the IEEE/CVF WACV*. 5689–5700.
- [54] Ramprasaath R Selvaraju, Michael Cogswell, Abhishek Das, Ramakrishna Vedantam, Devi Parikh, and Dhruv Batra. 2017. Grad-cam: Visual explanations from deep networks via gradient-based localization. In *Proceedings of the IEEE ICCV*. 618–626.
- [55] Fengyuan Shi, Ruopeng Gao, Weilin Huang, and Limin Wang. 2023. Dynamic mdetr: A dynamic multimodal transformer decoder for visual grounding. *IEEE Transactions on Pattern Analysis and Machine Intelligence* (2023).
- [56] Hwanjun Song, Minseok Kim, Dongmin Park, and Jae-Gil Lee. 2019. How does early stopping help generalization against label noise? *arXiv preprint arXiv:1911.08059* (2019).
- [57] Ben Sorscher, Robert Geirhos, Shashank Shekhar, Surya Ganguli, and Ari Morcos. 2022. Beyond neural scaling laws: beating power law scaling via data pruning. *Advances in Neural Information Processing Systems* 35 (2022), 19523–19536.
- [58] Wei Su, Peihan Miao, Huanzhang Dou, and Xi Li. 2024. Scanformer: Referring expression comprehension by iteratively scanning. In *Proceedings of the IEEE/CVF CVPR*. 13449–13458.
- [59] Wei Su, Peihan Miao, Huanzhang Dou, Gaoang Wang, Liang Qiao, Zheyang Li, and Xi Li. 2023. Language adaptive weight generation for multi-task visual grounding. In *Proceedings of the IEEE/CVF CVPR*. 10857–10866.
- [60] Jiamu Sun, Gen Luo, Yiyi Zhou, Xiaoshuai Sun, Guannan Jiang, Zhiyu Wang, and Rongrong Ji. 2023. Refteacher: A strong baseline for semi-supervised referring expression comprehension. In *Proceedings of the IEEE/CVF CVPR*. 19144–19154.
- [61] Mingjie Sun, Jimin Xiao, Eng Gee Lim, Si Liu, and John Y Goulermas. 2021. Discriminative triad matching and reconstruction for weakly referring expression grounding. *IEEE transactions on pattern analysis and machine intelligence* 43, 11 (2021), 4189–4195.
- [62] Yuxi Sun, Shanshan Feng, Xutao Li, Yunming Ye, Jian Kang, and Xu Huang. 2022. Visual grounding in remote sensing images. In *Proceedings of the 30th ACM International conference on Multimedia*. 404–412.
- [63] Saksham Suri, Fanyi Xiao, Animesh Sinha, Sean Culatana, Raghuraman Krishnamoorthi, Chenchen Zhu, and Abhinav Srivastava. 2024. Gen2Det: Generate to Detect. In *Synthetic Data for Computer Vision Workshop@ CVPR 2024*.
- [64] Tianyi Tang, Yushuo Chen, Yifan Du, Junyi Li, Wayne Xin Zhao, and Ji-Rong Wen. 2023. Learning to Imagine: Visually-Augmented Natural Language Generation. *arXiv preprint arXiv:2305.16944* (2023).
- [65] Yonglong Tian, Lijie Fan, Kaifeng Chen, Dina Katabi, Dilip Krishnan, and Phillip Isola. 2023. Learning vision from models rivals learning vision from data. *arXiv preprint arXiv:2312.17742* (2023).
- [66] Mariya Toneva, Alessandro Sordani, Remi Tachet des Combes, Adam Trischler, Yoshua Bengio, and Geoffrey J Gordon. 2018. An empirical study of example forgetting during deep neural network learning. *arXiv preprint arXiv:1812.05159* (2018).
- [67] Shijie Wang, Dahun Kim, Ali Taalimi, Chen Sun, and Weicheng Kuo. 2024. Learning Visual Grounding from Generative Vision and Language Model. *arXiv preprint arXiv:2407.14563* (2024).
- [68] Sai Wang, Yutian Lin, and Yu Wu. 2024. Omni-Q: Omni-Directional Scene Understanding for Unsupervised Visual Grounding. In *Proceedings of the IEEE/CVF CVPR*. 14261–14270.
- [69] Yibo Wang, Ruiyuan Gao, Kai Chen, Kaiqiang Zhou, Yingjie Cai, Lanqing Hong, Zhenguo Li, Lihui Jiang, Dit-Yan Yeung, Qiang Xu, et al. 2024. Dettiffusion: Synergizing generative and perceptive models for enhanced data generation and perception. In *Proceedings of the IEEE/CVF CVPR*. 7246–7255.
- [70] Dulanga Weerakoon, Vigneshwaran Subbaraju, Tuan Tran, and Archan Misra. 2022. SoftSkip: Empowering multi-modal dynamic pruning for single-stage referring comprehension. In *Proceedings of the 30th ACM International Conference on Multimedia*. 3608–3616.
- [71] Xiaobo Xia, Jiale Liu, Jun Yu, Xu Shen, Bo Han, and Tongliang Liu. 2022. Moderate coresets: A universal method of data selection for real-world data-efficient deep learning. In *The Eleventh International Conference on Learning Representations*.
- [72] Kai Xiao, Logan Engstrom, Andrew Ilyas, and Aleksander Madry. 2020. Noise or signal: The role of image backgrounds in object recognition. *arXiv preprint arXiv:2006.09994* (2020).
- [73] Linhui Xiao, Xiaoshan Yang, Xiangyuan Lan, Yaowei Wang, and Changsheng Xu. 2024. Towards Visual Grounding: A Survey. *arXiv preprint arXiv:2412.20206* (2024).
- [74] Linhui Xiao, Xiaoshan Yang, Fang Peng, Yaowei Wang, and Changsheng Xu. 2024. HiVG: Hierarchical Multimodal Fine-grained Modulation for Visual Grounding. *arXiv preprint arXiv:2404.13400* (2024).
- [75] Linhui Xiao, Xiaoshan Yang, Fang Peng, Ming Yan, Yaowei Wang, and Changsheng Xu. 2023. CLIP-VG: Self-paced Curriculum Adapting of CLIP for Visual Grounding. *IEEE Transactions on Multimedia* (2023).
- [76] Jiahao Xie, Wei Li, Xiangtai Li, Ziwei Liu, Yew Soon Ong, and Chen Change Loy. 2024. Mosaicfusion: Diffusion models as data augmenters for large vocabulary instance segmentation. *International Journal of Computer Vision* (2024), 1–20.
- [77] Sang Michael Xie, Shibani Santurkar, Tengyu Ma, and Percy S Liang. 2023. Data selection for language models via importance resampling. *Advances in Neural Information Processing Systems* 36 (2023), 34201–34227.
- [78] Yunyi Xuan, Weijie Chen, Shicai Yang, Di Xie, Luojun Lin, and Yueting Zhuang. 2023. Distilling Vision-Language Foundation Models: A Data-Free Approach via Prompt Diversification. In *Proceedings of the 31st ACM International Conference on Multimedia*. 4928–4938.
- [79] Han Xue, Zhiwu Huang, Qianru Sun, Li Song, and Wenjun Zhang. 2023. Freestyle layout-to-image synthesis. In *Proceedings of the IEEE/CVF CVPR*. 14256–14266.
- [80] Siming Yan, Min Bai, Weifeng Chen, Xiong Zhou, Qixing Huang, and Li Erran Li. 2024. Vigor: Improving visual grounding of large vision language models with fine-grained reward modeling. In *ECCV*. Springer, 37–53.
- [81] Lihe Yang, Xiaogang Xu, Bingyi Kang, Yinghuan Shi, and Hengshuang Zhao. 2024. Freemask: Synthetic images with dense annotations make stronger segmentation models. *Advances in Neural Information Processing Systems* 36 (2024).
- [82] Li Yang, Yan Xu, Chunfeng Yuan, Wei Liu, Bing Li, and Weiming Hu. 2022. Improving visual grounding with visual-linguistic verification and iterative reasoning. In *Proceedings of the IEEE/CVF CVPR*. 9499–9508.
- [83] Shuo Yang, Zeke Xie, Hanyu Peng, Min Xu, Mingming Sun, and Ping Li. 2022. Dataset pruning: Reducing training data by examining generalization influence. *arXiv preprint arXiv:2205.09329* (2022).
- [84] Yue Yang, Wenlin Yao, Hongming Zhang, Xiaoyang Wang, Dong Yu, and Jianshu Chen. 2022. Z-LaVi: Zero-Shot Language Solver Fueled by Visual Imagination. In *Proceedings of the 2022 Conference on Empirical Methods in Natural Language Processing*. 1186–1203.
- [85] Ziyang Yang, Kushal Kafle, Franck Derroncourt, and Vicente Ordonez. 2023. Improving visual grounding by encouraging consistent gradient-based explanations. In *Proceedings of the IEEE/CVF CVPR*. 19165–19174.
- [86] Zuhao Yang, Fangneng Zhan, Kunhao Liu, Muyu Xu, and Shijian Lu. 2023. AI-Generated Images as Data Source: The Dawn of Synthetic Era. *arXiv preprint arXiv:2310.01830* (2023).
- [87] Quanming Yao, Hansi Yang, Bo Han, Gang Niu, and James Tin-Yau Kwok. 2020. Searching to exploit memorization effect in learning with noisy labels. In *International Conference on Machine Learning*. PMLR, 10789–10798.
- [88] Ruilin Yao, Shengwu Xiong, Yichen Zhao, and Yi Rong. 2024. Visual Grounding with Multi-modal Conditional Adaptation. In *Proceedings of the 32nd ACM International Conference on Multimedia*. 3877–3886.
- [89] Fulong Ye, Yuxing Long, Fangxiang Feng, and Xiaojie Wang. 2023. Whether you can locate or not? Interactive Referring Expression Generation. In *Proceedings of the 31st ACM International Conference on Multimedia*. 4697–4706.
- [90] Jiabo Ye, Junfeng Tian, Ming Yan, Xiaoshan Yang, Xuwu Wang, Ji Zhang, Liang He, and Xin Lin. 2022. Shifting more attention to visual backbone: Query-modulated refinement networks for end-to-end visual grounding. In *Proceedings of the IEEE/CVF CVPR*. 15502.
- [91] Licheng Yu, Zhe Lin, Xiaohui Shen, Jimei Yang, Xin Lu, Mohit Bansal, and Tamara L Berg. 2018. MAttNet: Modular attention network for referring expression comprehension. In *Proceedings of the IEEE CVPR*. 1307–1315.
- [92] Licheng Yu, Patrick Poirson, Shan Yang, Alexander C Berg, and Tamara L Berg. 2016. Modeling context in referring expressions. In *ECCV 2016, Proceedings, Part II 14*. Springer, 69–85.
- [93] Xingrui Yu, Bo Han, Jiangchao Yao, Gang Niu, Ivor Tsang, and Masashi Sugiyama. 2019. How does disagreement help generalization against label corruption?. In *International Conference on Machine Learning*. PMLR, 7164.
- [94] Zhihan Yu and Ruifan Li. 2024. Revisiting counterfactual problems in referring expression comprehension. In *Proceedings of the IEEE/CVF CVPR*. 13438–13448.

- [95] Yunan Zeng, Yan Huang, Jinjin Zhang, Zequn Jie, Zhenhua Chai, and Liang Wang. 2024. Investigating compositional challenges in vision-language models for visual grounding. In *Proceedings of the IEEE/CVF CVPR*. 14141–14151.
- [96] Manlin Zhang, Jie Wu, Yuxi Ren, Ming Li, Jie Qin, Xuefeng Xiao, Wei Liu, Rui Wang, Min Zheng, and Andy J Ma. 2023. Diffusionengine: Diffusion model is scalable data engine for object detection. *arXiv preprint arXiv:2309.03893* (2023).
- [97] Haoyu Zhao, Wenhong Ge, and Ying-cong Chen. 2024. LLM-Optic: Unveiling the Capabilities of Large Language Models for Universal Visual Grounding. *arXiv preprint arXiv:2405.17104* (2024).
- [98] Hanqing Zhao, Dianmo Sheng, Jianmin Bao, Dongdong Chen, Dong Chen, Fang Wen, Lu Yuan, Ce Liu, Wenbo Zhou, Qi Chu, et al. 2023. X-paste: Revisiting scalable copy-paste for instance segmentation using clip and stablediffusion. In *International Conference on Machine Learning*. PMLR, 42098–42109.
- [99] Minghang Zheng, Jiahua Zhang, Qingchao Chen, Yuxin Peng, and Yang Liu. 2024. ResVG: Enhancing Relation and Semantic Understanding in Multiple Instances for Visual Grounding. In *Proceedings of the 32nd ACM International Conference on Multimedia*. 1187–1196.